Dilution-Induced Slow Magnetic Relaxation and Anomalous Hysteresis in Trigonal Prismatic Dysprosium(III) and Uranium(III) Complexes

ARTICLE *in* INORGANIC CHEMISTRY · AUGUST 2011

Dilution-Induced Slow Magnetic Relaxation and Anomalous Hysteresis in Trigonal Prismatic Dysprosium(III) and Uranium(III) Complexes

Katie R. Meihaus, Jeffrey D. Rinehart, and Jeffrey R. Long*

Department of Chemistry, University of California, Berkeley, Berkeley, California 94720, United States

S *Supporting Information*

ABSTRACT: Magnetically dilute samples of complexes Dy-$(H_2BPz^{Me2}_2)_3$ (**1**) and $U(H_2BPz_2)_3$ (**3**) were prepared through cocrystallization with diamagnetic $Y(H_2BPz^{Me2}_2)_3$ (**2**) and Y-$(H_2BPz_2)_3$. Alternating current (ac) susceptibility measurements performed on these samples reveal magnetic relaxation behavior drastically different from their concentrated counterparts. For concentrated **1**, slow magnetic relaxation is not observed under zero or applied dc fields of several hundred Oersteds. However, a 1:65 (Dy:Y) molar dilution results in a nonzero out-of-phase component to the magnetic susceptibility under zero applied dc field, characteristic of a single-molecule magnet. The highest dilution of **3** (1:90, U:Y) yields a relaxation barrier $U_{eff} = 16$ cm^{-1}, double that of the concentrated sample. These combined results highlight the impact of intermolecular interactions in mononuclear single-molecule magnets possessing a highly anisotropic metal center. Finally, dilution elucidates the previously observed secondary relaxation process for concentrated **3**. This process is slowed down drastically upon a 1:1 molar dilution, leading to butterfly magnetic hysteresis at temperatures as high as 3 K. The disappearance of this process for higher dilutions reveals it to be relaxation dictated by short-range intermolecular interactions, and it stands as the first direct example of an intermolecular relaxation process competing with single-molecule-based slow magnetic relaxation.
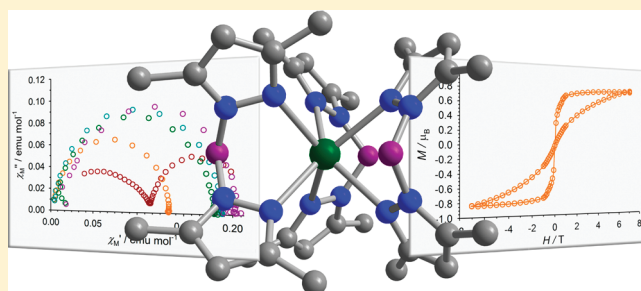
■ INTRODUCTION

Since the discovery of the first single-molecule magnet, $Mn_{12}O_{12}$-$(O_2CMe)_{16}(H_2O)_4$,[1] numerous other molecules have been shown to exhibit slow magnetic relaxation at sufficiently low temperatures.[2] Although the study of multinuclear transition metal clusters once dominated the field, observation of the same phenomenon in the lanthanide sandwich complexes $[LnPc_2]^{n+}$ (Ln = Dy, Tb, Ho; H_2Pc = phthalocyanine; $n = -1, 0, 1$)[3] has prompted increasing interest in mono- and multinuclear complexes incorporating 4f elements.[4] This direction holds considerable promise in view of the large unquenched orbital contribution to the moment and resulting high magnetic anisotropy that can arise for metal centers with open-shell f-electron configurations. Indeed, several important benchmarks for single-molecule magnets are held by lanthanide-based systems, including the largest anisotropy barrier[5] and the highest observed blocking temperature.[6] Actinide-containing molecules are of interest for similar reasons but have the added advantage of the greater radial extension of the valence 5f orbitals, which can allow for increased metal—ligand orbital overlap and larger crystal field splitting energies.[7] To date, however, only a very few actinide-based single-molecule magnets have been realized,[8−12] with the trigonal prismatic complexes $U(R_2BPz_2)_3$ (R = H, Ph; HPz = pyrazole) constituting two of the three examples utilizing the more easily handled element uranium.

With so few compounds characterized, especially for the actinides, significant gaps remain in our understanding of the mechanisms for slow magnetic relaxation in f-element single-molecule magnets. In particular, the multiple relaxation pathways displayed in several dysprosium[13] and actinide[9,11] systems have yet to be well understood. Additionally, the relaxation behavior for many lanthanide systems has been shown to vary significantly with applied field and upon dilution within a diamagnetic matrix.[3,13a,13e,14] Ishikawa and co-workers were the first to notice that dilution of $[LnPc_2]^-$ (Ln = Dy, Tb) led to a drastic shift in the frequency dependence of the ac magnetic susceptibility data. These results strongly suggest the importance of intermolecular magnetic dipolar interactions in influencing the relaxation in bulk crystalline samples. While this phenomenon has been studied in some detail in transition metal single-molecule magnets,[15] only recently has the impact of intermolecular effects begun to be investigated more thoroughly in f-element single-molecule magnets.[13a,e,14] Such studies are important because, while new studies are showing that the magnetic properties of isolated molecules can be addressed,[16] the majority of these are conducted on bulk samples wherein intermolecular interactions

must be accounted for. Because of this, acquiring a better understanding of intermolecular interactions and an ability to interpret their effects on molecular-based magnetic relaxation is crucial. Herein, we present a trigonal prismatic complex, $Dy(H_2BPz^{Me2}_2)_3$, that displays slow magnetic relaxation behavior under zero applied field only upon dilution within a diamagnetic matrix. These results further prompted us to re-examine the analogous complex $U(H_2BPz_2)_3$ in diluted forms, revealing a 2-fold increase in the single-molecule magnetic relaxation barrier as well as unprecedented evidence for magnetic hysteresis arising from intermolecular relaxation.

■ EXPERIMENTAL SECTION

General Considerations. All reactions and subsequent manipulations were performed under anaerobic and anhydrous conditions in a nitrogen atmosphere using a glovebox or Schlenk technique. THF, hexanes, and toluene were dried by passage over activated molecular sieves using a Vacuum Atmospheres solvent purification system. $U(H_2BPz_2)_3$, Y-$(H_2BPz_2)_3$, and $Y(H_2BPz^{Me2}_2)_3$ were prepared from literature procedures.[17,18] A modification of the method of Trofimenko[19] was used for the synthesis of dihydrobis(dimethylpyrazolyl)borate. UI_3 was prepared by modification of the method of Cloke and Hitchcock.[20] Fine uranium powder was prepared by synthesis of UH_3[21] and subsequent removal of hydrogen under dynamic vacuum at 400 °C. Heating of the fine metal powder with a stoichiometric amount of HgI_2 in a sealed tube at 320 °C for 2 days afforded the triiodide starting material. Anhydrous C_6D_6 was purchased from Cambridge Isotopes Laboratories, freeze–pump–thawed, and stored over activated 4 Å molecular sieves prior to use. 3,5-Dimethylpyrazole was purchased from Sigma Aldrich and purified by sublimation. Dihydrobis-(pyrazolyl)borate was purchased from Strem Chemicals and purified by recrystallization from THF/hexanes. NMR spectra were recorded on a Bruker AVB 400 or Bruker AV 300 spectrometer. IR spectra were recorded on a Perkin-Elmer Avatar Spectrum 400 FTIR Spectrometer equipped with ATR. Elemental analyses were performed by the Micro-Mass Facility at the University of California, Berkeley, on a Perkin-Elmer 2400 Series II combustion analyzer.

Synthesis of $Dy[H(\mu$-H$)BPz^{Me2}_2]_3$ (1). A THF solution of dihydrobis-(dimethylpyrazolyl)borate (0.30 g, 1.2 mmol) was added dropwise to a stirring slurry of $DyCl_3$ (0.11 g, 0.41 mmol) in THF (2 mL); the solution immediately developed a cloudy appearance. The mixture was stirred for 24 h, and THF was subsequently removed under reduced pressure. The resulting white powder was rinsed with hexanes, extracted into toluene (2 mL), and filtered over diatomaceous earth. Removal of the solvent resulted in spontaneous crystallization of a colorless solid in 46% yield (0.15 g). Layering of a toluene solution of 1 with hexanes (2:1/hexanes:toluene) and storage for 12 h at −20 °C afforded colorless rectangular plate-shaped crystals. ^{1}H NMR (300 MHz, 25 °C, C_6D_6): δ −38.22 (s, 18H, $\nu_{1/2}$ = 75 Hz, 3/5 Me), 21.02 (s, 6H, $\nu_{1/2}$ = 300 Hz, 4-H (Pz)), 146.79 (br s, 18H, $\nu_{1/2}$ = 600 Hz, 3/5 Me) IR (neat, cm^{-1}): 617 (m), 630 (m), 642 (w), 654 (w), 706 (w), 774 (s), 892 (w), 907 (w), 979 (w), 1041 (s), 1114 (s), 1166 (s), 1192 (s), 1236 (m), 1356 (s), 1374 (w), 1420 (s), 1451 (s), 1494 (w), 1536 (s); ν(B−H) 2220 (w), 2265 (w), 2296 (m), 2448 (m-s); 2931 (w), 2965 (w). Anal. Calcd for $C_{30}H_{48}B_3N_{12}Dy$: C, 46.69; H, 6.27; N, 21.77. Found: C, 46.92; H, 6.43; N, 21.65.

X-ray Structure Determination. Crystals of 2 were obtained from storing a saturated toluene solution at −20 °C for 12 h. Crystals of 1 and 2 were mounted on Kapton loops, transferred to a Brüker SMART diffractometer, and cooled in a nitrogen stream. The SMART program package was used to determine the unit cell parameters and for data collection (30 s/frame scan time for a hemisphere of diffraction data). Data integration was performed by SAINT software, and the absorption correction was provided by SADABS.[22] Subsequent calculations were carried out using the WinGX[23] program. The structures were solved by direct methods and refined against F^2 by full-matrix least-squares

techniques. The analytical scattering factors for neutral atoms were used throughout the analysis. Hydrogen atoms were included using a riding model. CCDC 820567 (1) and CCDC 820567 (2) contain the supplementary crystallographic data for this paper.[24] These data can be obtained free of charge from the Cambridge Crystallographic Data Center via www.ccdc.cam.ac.uk/data_request/cif.

Magnetic Measurements. Magnetic samples were prepared by adding crystalline powder compound to a 7 mm quartz tube with a raised quartz platform. Sufficient liquid eicosane (at 60 °C) was added to saturate and cover the samples to prevent crystallite torquing and provide good thermal contact between the sample and the bath. The tubes were fitted with Teflon sealable adapters, evacuated on a Schenk line or using a glovebox vacuum pump, and flame-sealed under vacuum. Interestingly, issues with sample torquing became more prevalent with greater dilutions.

Magnetic susceptibility measurements were collected using a Quantum Design MPMS2 SQUID magnetometer. Direct current susceptibility data measurements were performed at temperatures ranging from 2.0 to 300 K using an applied field of 1000 Oe. The amounts of 1 and 3 present in each dilute sample were confirmed by adjusting the mass of the paramagnetic material until the low-temperature portions of the dilute dc susceptibility curves overlapped with that of the neat compound (see Figure S2, Supporting Information). Alternating current magnetic susceptibility measurements were performed using a 4 Oe switching field. All data for 1 and 3 were corrected for diamagnetic contributions from the core diamagnetism estimated using Pascal's constants to give χ_D = −0.00041596 (1), −0.00040896 (2) −0.00030064 (3), −0.00026664 ($Y(H_2BPz_2)_3$), and −0.00024306 emu/mol (eicosane).

Temperature-dependent ac susceptibility measurements were performed at fields of 1000 Oe for 1 and 100 Oe for 3, at which fields the relaxation time reaches an approximate maximum for each compound. Dilution-dependent Cole−Cole plots for 3 were collected at an applied field of 4000 Oe, representing the optimum field at which the relaxation time is very large for the slower process and the faster process is simultaneously observable. Cole−Cole plots were fitted using formulas describing χ' and χ'' in terms of frequency, constant temperature susceptibility (χ_T), adiabatic susceptibility (χ_S), relaxation time (τ), and a variable representing the distribution of relaxation times (α).[2] All data fitted to α values of ≤0.38.

■ RESULTS AND DISCUSSION

The complex $Dy(H_2BPz^{Me2}_2)_3$ is readily synthesized from reaction of 3 equiv of the potassium salt of dihydrobis(dimethyl-pyrazolyl)borate $(H_2BPz^{Me2}_2{}^-)$ with $DyCl_3$ in THF. Colorless block-shaped crystals of $Dy(H_2BPz^{Me2}_2)_3 \cdot PhMe$ (1) suitable for X-ray analysis were grown from a concentrated solution of toluene layered with hexanes. The crystal structure of 1 revealed the expected trigonal prismatic complex geometry, which approaches D_{3h} point symmetry (see Figure 1). The diamagnetic yttrium analog of this compound has previously been synthesized,[18] although it was not structurally characterized. Crystals of $Y(H_2BPz^{Me2}_2)_3 \cdot PhMe$ (2) were grown from a concentrated solution of toluene and determined to be isostructural with 1. Dilute crystalline samples of 1 were prepared by cocrystallization with 2 from toluene in predetermined molar ratios.

The metal center in 1 has a similar ligand field environment to that in $U(H_2BPz_2)_3$,[9] yet the compound does not display slow magnetic relaxation, even under a dc field of several hundred Oe. We hypothesized that the much larger magnetic moment of Dy^{III} was contributing to internal magnetic fields that allowed for an anomalously fast relaxation pathway. To probe the influence of dipolar effects in this system, ac magnetic susceptibility measurements were performed on crystalline samples of $Dy_xY_{1−x}$-$(H_2BPz^{Me2}_2)_3 \cdot PhMe$ with Dy:Y molar ratios of 1:1 (53% Dy),
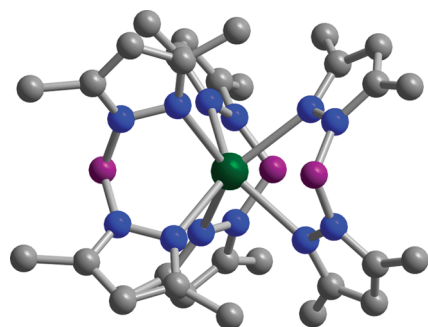
Figure 1. Structure of the trigonal prismatic complex $Dy(H_2BPz^{Me2}_2)_3$ as observed in **1**. Green, blue, gray, and purple spheres represent Dy, N, C, and B atoms, respectively; H atoms are omitted for clarity. A toluene molecule, not shown, cocrystallizes with the complex. Compound **2**, featuring the analogous complex $Y(H_2BPz^{Me2}_2)_3$, is isostructural. Selected interatomic distances (Å) and angles (deg) for **1** and **2**, respectively: Ln−N 2.450(3)−2.509(3), 2.453(3)−2.504(3); Ln···Ln 9.684, 9.583; N−Ln−N 77.8(1)−79.7(1), 77.75(9)−79.52(8).

1:15 (7% Dy), 1:65 (2% Dy), and 1:130 (1% Dy). With just a 1:1 dilution, slow relaxation of the magnetization is demonstrated through the appearance of an out-of-phase component to the susceptibility, χ'', at an applied field of 1000 Oe. This drastic slowing of the relaxation time attests to the significant role of nearest neighbor intermolecular interactions in speeding up the relaxation in undiluted **1**. Interestingly, in the 1:1 diluted phase, the χ'' signal appears to decrease and then increase again at the highest frequencies, suggesting the beginning of another out-of-phase peak and thus the presence of a second, faster relaxation process. For the 1:15 diluted sample, two significantly overlapping regions are indeed visible in the Cole−Cole plots at 1.8 K, and as the dilution increases these regions become better resolved within the frequency range measured (see Figures S4−S6, Supporting Information). The persistence of both of these relaxation regions at the highest dilution indicates that while intermolecular interactions clearly act to obscure the two processes, both arise from molecular-based relaxation in Dy-$(H_2BPz^{Me2}_2)_3$. As the temperature is increased, the faster process gradually moves beyond the high-frequency range of the magnetometer (<1500 Hz) and by 2.7 K only a single semicircle is observed in the Cole−Cole plot.

To establish whether the relaxation in **1** is thermally activated, the natural log of the relaxation, τ, for each dilution was plotted vs $1/T$ to check for Arrhenius-type linearity. Relaxation times and corresponding values of the α parameter[25] were extracted for the low-frequency peak by fitting Cole−Cole plots between 1.8 and 3.7 K using the generalized Debye model.[2] As seen in Figure 2 (top), the resulting plots follow Arrhenius behavior at high temperatures, attesting to the thermal dependence of this slow magnetic relaxation in **1**. Specifically, as the temperature is increased, a greater range of phonon modes is available to facilitate relaxation of the magnetic moment. Interestingly, while the high-temperature portions for the three highest dilutions nearly overlap, for a 1:1 dilution there is a distinct curvature at low temperatures. The relaxation time begins to level off at 2.5 K, the lowest temperature that can be fit for this dilution. For dilutions beyond 1:1, there is a much less pronounced low-temperature curvature and the relaxation time continues to lengthen, approaching the linear region defined at higher temperatures. Thus, this atypical temperature dependence of the
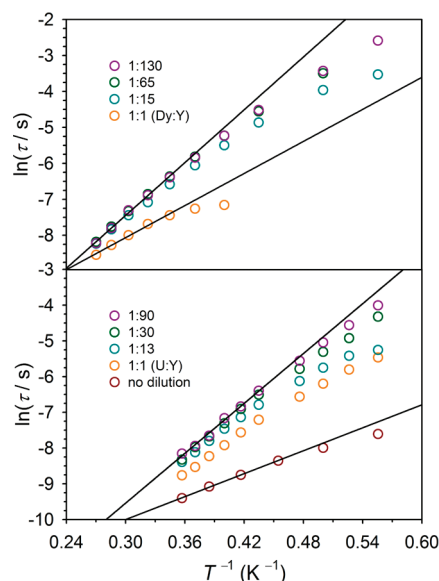

Figure 2. Plots of inverse temperature vs the natural log of the relaxation time for **1** (top) and **3** (bottom). Black lines represent fits to the Arrhenius expression $\ln(\tau) = \ln(\tau_0) + U_{eff}/k_BT$. Fitting the five and six highest temperature points for the highest dilutions of **1** and **3**, respectively, yields U_{eff} = 16/17 cm^{-1} and τ_0 = 4 × 10^{-7}/6 × 10^{-8} s.

relaxation in the 1:1 diluted sample indicates that intermolecular interactions are strong enough to persist for **1**, even after eliminating the nearest neighboring spins in the lattice.

With each dilution, the thermally activated relaxation barrier increases with a concomitant decrease in τ_0, again confirming that removal of intermolecular interactions leads to slower molecular relaxation. A dilution of 1:65 (Dy:Y) even results in a visible out-of-phase signal under no applied field at 1.7 and 1.8 K; however, χ'' does not reach a maximum until beyond the high-frequency limit of our magnetometer (see Figure S7, Supporting Information). Upon even greater dilution (1:130), there is no further shift of the χ'' signal to lower frequencies under zero or applied field and the Arrhenius plot remains essentially unchanged. Thus, for an ion−ion separation of approximately 23 Å, corresponding to 1:65 dilution, we appear to reach the limit of the interior interactions for this molecule. While the final U_{eff} of 17 cm^{-1} extracted for this highest dilution is small compared to other lanthanide single-molecule magnets, the significance of compound **1** is found not in the barrier but in its transformation from a simple paramagnetic solid to a zero-field single-molecule magnet simply through diamagnetic dilution. The results further suggest that mononuclear lanthanide single-molecule magnets may be more common than previously realized but that intermolecular interactions in these systems may be masking the presence of slow magnetic relaxation. It should be noted that the large distance between metal centers and the lack of a feasible exchange pathway through the bis(pyrazolyl)borate ligand precludes the existence of an exchange interaction that might contribute to the observed dilution dependence of the relaxation. The same is true of $U(H_2BPz_2)_3$ (vida infra) where the closest interion spacing is 8.167 Å.

In light of the above results, we were eager to study the impact of dilution on $U(H_2BPz_2)_3$ (**3**), which similarly displays no ac signal under zero applied field as well as multiple relaxation processes. Crystalline samples of **3** diluted in a diamagnetic matrix of $Y(H_2BPz_2)_3$[18] were prepared in U:Y molar ratios of
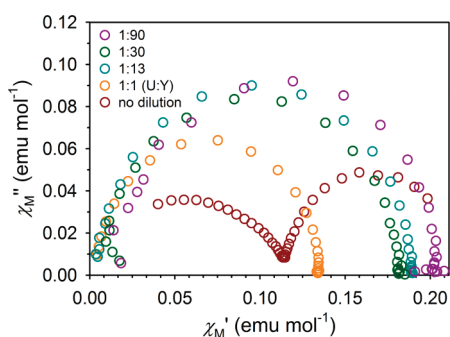
Figure 3. Cole—Cole plots for **3** at 1.8 K and an applied field of 4000 Oe. In the undiluted compound, the fast (left) and slow (right) processes are both visible; however, the slower process moves out of the time scale of the ac measurement upon 1:1 dilution.

Figure 4. Variable-field magnetization data for the 1:1 diluted compound $U_{0.5}Y_{0.5}(H_2BPz_2)_3$. The solid line serves as a guide for the eye.

1:1 (56% U), 1:13 (9% U), 1:30 (4% U), and 1:90 (1% U). The study of samples with larger dilution ratios was precluded by instrument sensitivity. Alternating current magnetic susceptibility data collected under a dc field of 100 Oe reveal a drastic dilution dependence of the relaxation time, as observed in the frequency dependence of the out-of-phase susceptibility, χ'' (see Figure S8, Supporting Information). At 1.8 K, a 1:1 dilution leads to a shift in χ'' of nearly 2 orders of magnitude from the undiluted sample and the out-of-phase signal continues to shift to lower frequencies with increasing dilution. The effect of dilution on the temperature dependence of the relaxation in **3** can be seen quantitatively in Figure 2 (bottom), where the natural log of the relaxation time is plotted versus $1/T$ for each dilution over the range 1.8—2.8 K at an applied field of 100 Oe.

As is evident from Figure 2, the impact of dilution on the temperature-dependent relaxation in **3** is even more drastic than for **1**. A 1:1 dilution leads to a significant increase in the slope of the Arrhenius plot, which continues to increase with dilution, as does the relaxation time at each temperature. Fitting the six highest temperature points of the 1:90 diluted sample to an Arrhenius law yields values of $U_{eff} = 16$ cm^{-1} and $\tau_0 = 6 \times 10^{-8}$ s. This barrier is two times that originally determined for the undiluted compound, and moreover, τ_0 has decreased by 2 orders of magnitude, closely approaching the normal range for a single-molecule magnet.[2] Clearly in **3**, as in **1**, intermolecular dipolar interactions play a very significant role in speeding up molecular-based slow magnetic relaxation.

Our previous investigation of the dynamic magnetism of undiluted **3** revealed the presence of two well-separated relaxation processes in Cole—Cole plots at dc fields as low as 1000 Oe.[9] The faster relaxation was ascribed to a thermally activated process, in accordance with its demonstrated temperature dependence. The slower process proved to relax independently of temperature in the measured range of 1.8—3.0 K, however, and the limited temperature range of the observed signal allowed only a qualitative analysis of potential relaxation mechanisms. In pursuit of a further understanding of this slower relaxation process and in order to discern the influence of dilution on both processes, ac susceptibility data were collected for dilute samples at 1.8 K and an applied field of 4000 Oe. The Cole—Cole plots for each dilution are shown together in Figure 3 with the undiluted data in red symbols for comparison. Upon a 1:1 dilution, the slower process is no longer visible within the frequency range probed (0.06—1500 Hz), suggesting that relaxation has slowed down so drastically that it has moved completely
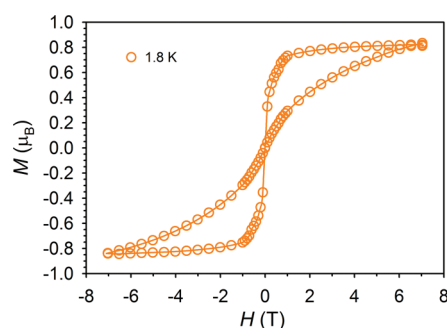
out of the ac time scale. To test this possibility, variable-field magnetization measurements were performed, revealing a magnetic hysteresis loop that, although closed at zero field, remains open at higher fields up to 3 K (see Figures 4 and S9, Supporting Information).

Given the small barrier for the temperature-dependent relaxation observed in the ac measurements, the hysteresis must be ascribed to the much slower process originally observed in undiluted **3**. Analysis of the hysteresis shape reveals a strong field dependence for this process. The loop displays no remnant magnetization as the moment of the sample rapidly plummets to zero upon removal of the field. Analysis of the Cole—Cole plots in Figure 3 at higher dilutions shows that the corresponding isothermal susceptibility values, χ_T, differ from the value of χ_{dc} by no more than 0.1 emu/mol, which is within the variation of the diluted dc values from the undiluted sample (see Figure S2, bottom, Supporting Information). Thus, no significant component of χ' remains unaccounted for at these higher dilutions. Interestingly, variable-field magnetization data for the 1:13 diluted sample do reveal hysteretic behavior at 1.8 K, although the loop opens only between 1 and 2.5 T and is closed at higher temperatures. Hysteresis is completely shut down for higher dilutions. Thus, a 1:1 dilution yields an optimum ion—ion separation for slowing down the relaxation occurring for this slower process.

These results suggest that the slower relaxation process is not single-molecule based, for if that were the case the hysteresis should only become more prominent upon increasing dilution and the corresponding removal of dipolar interactions. Conversely, we observe that higher dilutions actually suppress the hysteresis and lead to its ultimate disappearance; thus, this slow relaxation is intermolecular in origin. It must be stressed, however, that there is an important difference between this slow intermolecular relaxation and the interactions causing artificially fast molecular relaxation in both **3** and **1**. In the latter case, intermolecular interactions are merely inferred from changes in molecular relaxation data upon magnetic dilution (Figure 2 and previous magnetic dilution studies[3,13a,13e,14]). Moreover, such interactions can be mitigated by magnetic dilution. The slow process described here, however, reveals an intermolecular relaxation that is actually strengthened by increasing the magnetic ion separation. We attributed this very slow relaxation in **3** to a collective spin relaxation brought about by short-range intermolecular ordering. Only the faster relaxation at high frequencies in **3**, which becomes dominant upon dilution of the spins, may be ascribed to a molecular process. Analogies for this slower process can be drawn from paramagnetic relaxation

studies performed on the compounds $Ln(OH)_3$ (Ln = Tb, Dy, Ho),[26] dysprosium ethyl sulfate ($Dy(CH_3CH_2SO_4)_3 \cdot 9H_2O$, DyEtS),[27] and terbium arsonate[28] starting in the 1960s. In these systems, two relaxation domains are also apparent at low temperatures, albeit on a much faster time scale. The low-frequency relaxation in these systems was attributed to domain wall movement, and while the probed frequencies and temperatures differ significantly from those in our study, it is easy to draw analogies between **3** and salts such as DyEtS. Each is a molecular solid, and the smallest interion spacings in undiluted **3** are comparable to those in DyEtS (8.167(2) vs 7.0122(6) Å). Thus, the distinction between "ferromagnetic solid" and single-molecule magnet becomes blurred.

We are aware of only two related examples in the f-element single-molecule magnet literature for butterfly hysteresis observed in conjunction with multiple relaxation processes, and these involve neptunocene ($Np(COT)_2$; COT^{2-} = cyclooctatetraenide)[11] and the dysprosium complex $[Dy(acac)_3(H_2O)_2]$.[13e] In neptunocene, hysteresis is observable at 1.8 K and fields above 5 T, and this relaxation is ascribed to a process dominant at high fields and distinct from a faster, low-field process for which a relaxation barrier of $U_{eff} = 28$ cm^{-1} was extracted. Both relaxation processes are assumed to be molecular; however, they are not found to occur on a similar time scale, as observed in undiluted **3**. For $[Dy(acac)_3(H_2O)_2]$, butterfly magnetic hysteresis is apparent at 0.5 K in the undiluted compound and at as high as 2 K upon dilution. Notably, the hysteresis loop widens with a 1:20 dilution but shrinks again upon further dilution. Further experimentation may elucidate whether the type of slow collective spin relaxation occurring in **3** may also take part in the relaxation occurring in these other systems.

■ CONCLUSIONS

The foregoing results clearly demonstrate the significant impact of dipolar interactions in two f-element-based mononuclear single-molecule magnets and reveal that such interactions have the potential to facilitate a relaxation phenomenon that might readily be mistaken as molecular in origin. In the case of **1**, intermolecular interactions of the kind studied in previous literature are evidenced to be strong enough to completely disable the slow molecular relaxation pathways in the magnetically concentrated sample. However, upon magnetic dilution, single-molecule magnet behavior is revealed, extending even to zero-field slow relaxation. In **3**, magnetic dilution leads to a nearly 100-fold increase in the molecular relaxation time, revealing another single-ion system in which intermolecular interactions hinder molecular relaxation. Perhaps most interesting is the discovery of a collective relaxation process arising from dipolar interactions, being distinct from previously observed intermolecular effects and leading to magnetic hysteresis observable up to 3 K. These results further highlight the importance of understanding the factors that moderate slow magnetic relaxation for mononuclear single-molecule magnets with unquenched orbital moment and high anisotropy. In particular, where intermolecular interactions are prevalent, such effects can lead to artificially small relaxation barriers or promote relaxation behavior such as magnetic hysteresis. Importantly, the latter effect can easily be misattributed to the individual molecule. Further understanding these effects is crucial to accurately reporting the molecular magnetic properties, as opposed to ensemble properties. With an eye toward the future of possibly constructing single-molecule magnet memory storage and computing devices, the study of intermolecular relaxation

effects is particularly critical, since dipolar interactions can heavily influence quantum coherence times.[29]

■ AUTHOR INFORMATION

Corresponding Author
*E-mail: jrlong@berkeley.edu.

■ REFERENCES

(1) (a) Sessoli, R.; Tsai, H. L; Schake, A. R.; Wang, S.; Vincent, J. B.; Folting, K.; Gatteschi, D.; Christou, G.; Hendrickson, D. N. *J. Am. Chem. Soc.* **1993**, *115*, 1804–1816. (b) Sessoli, R.; Gatteschi, D.; Caneschi, A.; Novak, M. A. *Nature* **1993**, *365*, 141–143.

(2) Gatteschi, D.; Sessoli, R.; Villain, J. *Molecular Nanomagnets*; Oxford University Press: New York, 2006.

(3) Ishikawa, N.; Sugita, M.; Ishikawa, T.; Koshihara, S.-y.; Kaizu, Y. *J. Am .Chem. Soc.* **2003**, *125*, 8694–8695.

(4) (a) Long, J.; Habib, F.; Lin, P.-H.; Korobkov, I.; Enright, G.; Ungur, L.; Wernsdorfer, W.; Chibotaru, L. F.; Murugesu, M. *J. Am. Chem. Soc.* **2011**, *133*, 5319–5328. (b) Jiang, S.-D.; Wang, B.-W.; Sun, H.-L.; Wang, Z.-M.; Gao, S. *J. Am. Chem. Soc.* **2011**, *133*, 4730–4733. (c) Gao, Y.; Zhao, L.; Xu, X.; Xu, G.-F.; Guo, Y.-N.; Tang, J.; Liu, Z. *Inorg. Chem.* **2011**, *50*, 1304–1308. (d) Feltham, H. L. C.; Clérac, R.; Powell, A. K.; Brooker, S. *Inorg. Chem.* **2011**, *50*, 4232–4234. (e) Kajiwara, T.; Nakano, M.; Takahashi, K.; Takaishi, S.; Yamashita, M. *Chem.—Eur. J.* **2011**, *17*, 196–205. (f) Pointillart, F.; Bernot, K.; Sessoli, R.; Gatteschi, D. *Inorg. Chem.* **2010**, *49*, 4355–4361. (g) Yamaguchi, T.; Costes, J.-P.; Kishima, Y.; Kojima, M.; Sunatsuki, Y.; Bréfuel, N.; Tuchagues, J.-P.; Vendier, L.; Wernsdorfer, W. *Inorg. Chem.* **2010**, *49*, 9125–9135. (h) Kajiwara, T.; Yakahashi, K.; Hiraizumi, T.; Takaishi, S.; Yamashita, M. *Polyhedron* **2009**, *28*, 1860–1863. (i) Sessoli, R.; Powell, A. K. *Coord. Chem. Rev.* **2009**, *253*, 2328–2341. (j) Lin, P.-H.; Burchell, T. J.; Ungur, L.; Chibotaru, L. F.; Wernsdorfer, W.; Murugesu, M. *Angew. Chem., Int. Ed.* **2009**, *48*, 9489–9492.

(5) Takamatsu, S.; Ishikawa, T.; Koshihara, S.; Ishikawa, N. *Inorg. Chem.* **2007**, *46*, 7250–7252.

(6) Rinehart, J. D.; Fang, M.; Evans, W. J.; Long, J. R. *Nat. Chem.* **2011**, *3*, 538–542.

(7) Rinehart, J. D.; Harris, T. D.; Kozimor, S. A.; Bartlett, B. M.; Long, J. R. *Inorg. Chem.* **2009**, *48*, 3382–3395.

(8) Rinehart, J. D.; Long, J. R. *J. Am. Chem. Soc.* **2009**, *131*, 12558–12559.

(9) Rinehart, J. D.; Meihaus, K. R.; Long, J. R. *J. Am. Chem. Soc.* **2010**, *132*, 7572–7573.

(10) Magnani, N.; Colineau, E.; Eloirdi, R.; Griveau, J.-C.; Caciuffo, R. *Phys. Rev. Lett.* **2010**, *104*, 197202.

(11) Magnani, N.; Apostolidis, C.; Morgenstern, A.; Colineau, E.; Griveau, J.-C.; Bolvin, H.; Walter, O.; Caciuffo, R. *Angew. Chem., Int. Ed.* **2011**, *50*, 1696–1698.

(12) Mills, D. P.; Moro, F.; McMaster, J.; van Slageren, J.; Lewis, W.; Blake, A. J.; Liddle, S. T. *Nat. Chem.* **2011**, *3*, 454–460.

(13) (a) Car, P.-E.; Perfetti, M.; Mannini, M.; Favre, A.; Caneschi, A.; Sessoli, R. *Chem. Commun.* **2011**, *47*, 3751–3753. (b) Katoh, K.;

Kajiwara, T.; Nakano, M.; Nakazawa, Y.; Wernsdorfer, W.; Ishikawa, N.; Breedlove, B. K.; Yamashita, M. *Chem.—Eur. J.* **2011**, *17*, 117–122. (c) Gonidec, M.; Luis, F.; Vílchez, À.; Esquena, J.; Amabilino, D. B.; Veciana, J. *Angew. Chem., Int. Ed.* **2010**, *49*, 1623–1626. (d) Hewitt, I. J.; Tang, J.; Madhu, N. T.; Anson, C. E.; Lan, Y.; Luzon, J.; Etienne, M.; Sessoli, R.; Powell, A. K. *Angew. Chem., Int. Ed.* **2010**, *49*, 6352–6356. (e) Jiang, S.-D.; Wang, B.-W.; Su, G.; Wang, Z.-M.; Gao, S. *Angew. Chem., Int. Ed.* **2010**, *49*, 7448–7451. (f) Guo, Y.-N.; Xu, G.-F.; Gamez, P.; Zhao, L.; Lin, S.-Y.; Deng, R.; Tang, J.; Zhang, H.-J. *J. Am. Chem. Soc.* **2010**, *132*, 8538–8539.

(14) (a) Habib, F.; Lin, P.-H.; Long, J.; Korobkov, I.; Wernsdorfer, W.; Murugesu, M. *J. Am. Chem. Soc.* **2011**, *133*, 8830–8833. (b) Luis, F.; Martínez-Pérez, M. J.; Montero, O.; Coronado, E.; Cardona-Serra, S.; Martí-Gastaldo, C.; Clemente-Juan, J. M.; Sesé, J.; Drung, D.; Schurig, T. *Phys. Rev. B* **2010**, *82*, 060403. (c) Layfield, R. A.; McDouall, J. J. W.; Sulway, S. A.; Tuna, F.; Collison, D.; Winpenny, R. E. P. *Chem.—Eur. J.* **2010**, *16*, 4442–4446. (d) Lin, P.-H.; Burchell, T. J.; Clérac, R.; Murugesu, M. *Angew. Chem., Int. Ed.* **2008**, *47*, 8848–8851. (e) Ishikawa, N.; Sugita, M.; Ishikawa, T.; Koshihara, S.-y.; Kaizu, Y. *J. Phys. Chem. B* **2004**, *108*, 11265–11271.

(15) (a) Wernsdofer, W.; Bhaduri, S.; Tiron, R.; Hendrickson, D. N.; Christou, G. *Phys. Rev. Lett.* **2002**, *89*, 197201–1 – 197201–4. (b) Affronte, M.; Lasjaunias, J. C.; Wernsdorfer, W.; Sessoli, R.; Gatteschi, D.; Heath, S. L.; Fort, A.; Rettori, A. *Phys. Rev. B* **2002**, *66*, 064408–1–064408–7. (c) Wernsdorfer, W.; Caneschi, A.; Sessoli, R.; Gatteschi, D.; Cornia, A.; Villar, V.; Paulsen, C. *Phys. Rev. Lett.* **2000**, *84*, 2965–2968. (d) Wernsdorfer, W.; Ohm, T.; Sangregorio, C.; Sessoli, R.; Mailly, D.; Paulsen, C. *Phys. Rev. Lett.* **1999**, *82*, 3903–3906. (d) Prok'ev, N. V.; Stamp, P. C. E. *Phys. Rev. Lett.* **1998**, *80*, 5794–5797.

(16) (a) Candini, A.; Klyatskaya, S.; Ruben, M.; Wernsdorfer, W.; Affronte, M. *Nano Lett.* **2011**, *11*, 2634–2639. (b) Sanvito, S. *Nat. Mater.* **2011**, *10*, 484–485. (c) Uradampilleta, M.; Klyatskaya, S.; Kleuziou, J.-P.; Wernsdorfer, W. *Nat. Mater* **2011**, *10*, 502–506. (d) Bogani, L.; Wernsdorfer, W. *Nat. Mater.* **2008**, *7*, 179–186. (e) Vitali, L.; Fabris, S.; Conte, M. A.; Brink, S.; Ruben, M.; Baroni, S.; Kern, K. *Nano Lett.* **2008**, *8*, 3364–3368.

(17) Sun, Y.; Takats, J.; Eberspacher, T.; Day, V. *Inorg. Chim. Acta* **1995**, *229*, 315–322.

(18) Reger, D. A.; Lindeman, J. A.; Lebioda, L. *Inorg. Chem.* **1988**, *27*, 1890–1896.

(19) Trofimenko, S. *J. Am. Chem. Soc.* **1967**, *89*, 6288–6294.

(20) Cloke, F. G. N.; Hitchcock, P. B. *J. Am. Chem. Soc.* **2002**, *124*, 9352–9353.

(21) Spedding, F. H.; Newton, A. S.; Warf, J. C.; Johnson, O.; Nottorf, R. W.; Johns, I. B.; Daane, A. H. *Nucleonics* **1949**, *4*, 4–15.

(22) Sheldrick, G. M. *SADABS*, Version 2.03; Bruker Analytical X-Ray Systems, Inc: Madison, WI, 2000.

(23) Farrugia, L. J. *J. Appl. Crystallogr.* **1999**, *32*, 837–838.

(24) Crystal data for **1**: colorless crystals, monoclinic, $P2(1)/n$, $a = 11.7325(10)$ Å, $b = 12.3614(11)$ Å, $c = 29.351(3)$ Å, $\alpha = 90°$, $\beta = 92.0510(10)°$, $\gamma = 90°$, $V = 4254.0(6)$ Å^3, $Z = 4$, formula = $C_{37}H_{48}B_3DyN_{12}$, $M_r = 855.80$, $\rho(\text{calcd}) = 1.336$ Mg/m^3, cryst dimens $= 0.52 \times 0.15 \times 0.06$ mm^3, $\mu = 1.797$ mm^{-1}, Mo Kα radiation ($\lambda = 0.7$ Å), $T = 127(2)$ K, $2\theta_{max} = 1.7996$, residual electron density = 1.176, measd reflns = 40 317, independent reflns = 7806, $R(\text{int}) = 0.0347$, R1 = 0.0316 ($I > 2\sigma(I)$), wR2 = 0.0853 (all data), 443 parameters, 15 restraints. Crystal data for **2**: colorless crystals, monoclinic, $P2(1)/n$, $a = 11.704(5)$ Å, $b = 12.442(5)$ Å, $c = 29.007(5)$ Å, $\alpha = 90.000(5)°$, $\beta = 91.263(5)°$, $\gamma = 90.000(5)°$, $V = 4223(3)$ Å^3, $Z = 4$, formula = $C_{37}H_{56}B_3N_{12}Y$, $M_r = 790.28$, $\rho(\text{calcd}) = 1.243$ Mg/m^3, cryst dimens = $0.07 \times 0.04 \times 0.03$ mm^3, $\mu = 1.422$ mm^{-1}, Mo Kα radiation ($\lambda = 0.7$ Å), $T = 156(2)$ K, $2\theta_{max} = 1.9172$, residual electron density = 0.554, measd reflns = 57 343, independent reflns = 7721, $R(\text{int}) = 0.0447$, R1 = 0.0447 ($I > 2\sigma(I)$), wR2 = 0.1268 (all data), 496 parameters, 0 restraints

(25) The α value determines the distribution of the relaxation times. An α value of zero indicates a single relaxation time while a value of one indicates an infinite distribution of relaxation times. The α values corresponding to the temperature dependent relaxation times for **1**

were within the range of 0.103−0.38 (Table S1, Supporting Information), revealing a narrow to moderate distribution of relaxation times in agreement with the presence of molecular relaxation influenced by intermolecular interactions.

(26) Schlachetzki, A.; Eckert, J. *Phys. Status Solidi (A)* **1972**, *11*, 611–622.

(27) Cooke, A. H.; Edmonds, D. T.; Finn, C. B. P.; Wolfe, W. P. *Proc. R. Soc. A* **1968**, *306*, 335–353.

(28) Müller, P. H.; Kasten, A.; Schienle, M. *Phys. Status Solidi (B)* **1983**, *119*, 239–249.

(29) Stamp, P. C. E.; Gaita-Ariño, A. *J. Mater. Chem.* **2009**, *19*, 1718–1730.

8489

dx.doi.org/10.1021/ic201078r |*Inorg. Chem.* 2011, 50, 8484–8489